Chinese Journal of Aeronautics 25 (2012) 57-63

Contents lists available at ScienceDirect

Chinese Journal of Aeronautics

journal homepage: www.elsevier.com/locate/cja

Imaging of the Space-time Structure of a Vortex Generator in Supersonic Flow

WANG Dengpan, XIA Zhixun*, ZHAO Yuxin, WANG Bo, ZHAO Yanhui

Science and Technology on Scramjet Laboratory, National University of Defense Technology, Changsha 410073, China

Received 15 June 2011; revised 15 August 2011; accepted 29 August 2011

Abstract

The fine space-time structure of a vortex generator (VG) in supersonic flow is studied with the nanoparticle-based planar laser scattering (NPLS) method in a quiet supersonic wind tunnel. The fine coherent structure at the symmetrical plane of the flow field around the VG is imaged with NPLS. The spatial structure and temporal evolution characteristics of the vortical structure are analyzed, which demonstrate periodic evolution and similar geometry, and the characteristics of rapid movement and slow change. Because the NPLS system yields the flow images at high temporal and spatial resolutions, from these images the position of a large scale structure can be extracted precisely. The position and velocity of the large scale structures can be evaluated with edge detection and correlation algorithms. The shocklet structures induced by vortices are imaged, from which the generation and development of shocklets are discussed in this paper.

Keywords: vortex generator; nanoparticle-based planar laser scattering; vortical structure; evolution characteristic; shocklet

1. Introduction

The vortex generator (VG) is an important flow-controlling component widely used in the field of aviation, aerospace, automobile, chemical engineering, and other fields. The VG induces complex vortical structures by flowing over a body, which affects the dynamic characteristics of the controlled flow. The flow structures of VGs in supersonic flow field are very complex, in that the influences of compressibility, shock wave and turbulence, and the corresponding evolution in time and space have not reached a consensus yet. For conventional VGs, the height is usually the same or slightly higher than the thickness of the boundary layer. However, some problems such as the induced drag and the disturbance to mainstream limit their application, which in fact has promoted the VG to miniaturization [1]. The VG jets developed recently exhibit good performances in structural stability and non-design state. However, although VG jets can overcome some defects of the conventional VG, the large demand for jet mass flow also restricts its application [2-3]. Many attractions were given to the flow-controlling of vortex generation in low Mach number flow [4]. Angele, et al. [5] studied the instantaneous flow filed of vortex generation in low Mach number flow, and found that the spirals caused by a VG were in unsteady states. Ola, et al. [6] investigated the control of traditional vane-type VG for the separation of boundary layers of low Mach number turbulent flat plates. Micro-VGs have a broad application prospect in the design of supersonic or hypersonic inlets, and the heights occupy only 10%-70% of the thicknesses of the boundary layers [7]. Both the device parasitic resistance and the extra cost due to nondesign state were reduced when compared with the conventional VGs. Moreover, VGs are also used in the forced transition of boundary layers, such as in the former-boundary layer transition experiment of X-43 trial aircraft [8] for their good effect.

Detailed studies on the wake field of various micro-

*Corresponding author. Tel.: +86-29-88493009.
*E-mail address:*xiazhixun@sina.com
Foundation item: National Natural Science Foundation of China (11072264)

doi: 10.1016/S1000-9361(11)60362-2

VGs were proceeded in order to increase the understanding of their controlling effects in fluid control, and optimize their sizes and installation locations. Charles, et al. [9] compared the flow structures of different micro-ramp sizes by using such techniques as schlieren, oilflow, wall pressure's measurement, laser Doppler anemometer (LDA) and so on. They suggested that the mechanism of micro-ramp was due to the fact that it could induce a relatively stronger reverse rotating streamwise vortex in the mainstream, and produce a blending effect in the boundary layers. They also found that the developing modes in downstream low momentum regions were very similar to micro-ramps with different sizes. Their conclusions were to some extent proved by Ref. [10] through the basic structure of flow file obtained by numerical simulation. Blinde, et al. [11] studied the fine structure of downstream for micro-ramp at Mach number $Ma = 1.84$ by stereoscopic particle image velocimetry (PIV) technique, and investigated the control effects of the single row and double rows micro-ramp matrix to the shock wave/boundary layer interaction (SWBLI). Based on the Reynolds-averaged Navier-Stokes (RANS) simulation, Anderson, et al. [12] optimized the configu- retion parameters of three kinds of VGs at $Ma = 2.0$ through the design of experiments (DOE) method of response surface modeling.

The present study uses the high temporal and spatial resolution NPLS technique in a quiet supersonic wind tunnel to study the space-time evolution and the dynamical characteristics of coherent structures about VGs [13-14].

2. Experimental Facility and Condition

2.1. Quiet supersonic wind tunnel

Because of the compressibility, strong discontinuity and strong non-linearity of the supersonic flow field, its dynamic mechanism is far more complicated than a low Mach number incompressible flow field. In order to guarantee the supersonic flow quality and avoid the influence of clutter on the experimental study of the flow around the VG and fine vortical structure, all experiments were conducted in National University of Defence Technology (NUDT) KD-02 quiet supersonic wind tunnel. The test section and nozzle of this wind tunnel were designed with characteristics to ensure the resultant flow field being laminar.

The wind tunnel was mainly composed of the upstream transition section, stability section, test section, nozzle and downstream vacuum tank system. A heavy caliber transition section is used to collect air from the ambient atmosphere into the upstream section, through which the inflow has lower velocity, better uniformity and lower turbulence. The airflow quality is obviously improved after the inflow passed through the rectifying equipment and experienced a long dissipation in the stability section, which is was helpful to achieve laminar flow in the downstream of the nozzle. The air-breathing quiet supersonic wind tunnel had lower total pressure and smaller Reynolds number in the experiment section than the blow-down wind tunnel, which helped to realize the laminarization of the nozzle. The nozzle and test section were integrated to avoid flow disturbance from installation errors. The sidewalls of the experiment section was designed with large observing windows to enable optical observation from all directions. The experimental section is 400 mm in length, 200 mm in height, and 200 mm in width. The width of the experimental section was designed as large as possible in order to effectively reduce the effect of a sidewall on the mainstream. The incident point of the reflected shock waves of the VG from sidewalls was out of the observation area. The calibrated Mach number of the wind tunnel is 2.68, the total pressure of inflow is 1.013×10^5 Pa, and the total temperature is 300 K. Figure 1 shows the photograph of the quite supersonic wind tunnel.

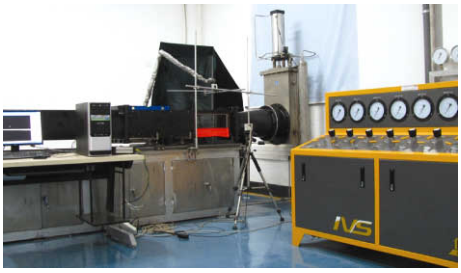

Fig. 1 Experiment facility of quiet supersonic wind tunnel.

2.2. NPLS experiment technique

The NPLS is a new technique for flow visualization, which uses nanoparticles as the tracer particles. Due to the high spatial and temporal resolutions and high signal-to-noise ratio (SNR) [14], the NPLS can clearly show the fine vortical structure in a turbulent boundary layer, and directly manifest the peripheral flow field structure of VG and its effect on the turbulent boundary layer.

The NPLS system used here is similar to the system developed by Zhao, et al [14]. The illumination is a double-pulsed Nd:YAG laser, with output wavelength 532 nm, and pulse energy 350 mJ at 6 ns. The actual exposure time of the camera is the same as the laser pulse by utilizing a filtering instrument. The instantaneous structures of the supersonic flow field will be taken. The imaging device we used is an IMPERX digital camera, equipped with a NIKON 105 mm lens. The maximum magnification is 1:1, and the resolution of the CCD (Charge Coupled Device) is $4\,096 \times 2\,600$ pixels. Two frames will be captured through an external trigger, and the captured image data will be transmitted in real time to a computer memory by the image acquisition board. The trigger signal is provided by a synchronous controller, which can thus keep synchronous with the pulse laser. Tracing the flow with nanoparticles is the core of NPLS, A NUDT KD-5 nanoparticle generator is used in this study. The

calibrated experiments prove that the average diameter of generated nanoparticles is about 45 nm with good flow-following ability. The changes in speed and density in the flow field will directly influence the concentration of nanoparticles and thus cause changed gray scale of images.

Figure 2 is the schematic of NPLS experiment system [13]. In NPLS, a computer controls the collaboration of every component and receives the experimental images. The input and output parameters of the synchronizer are controlled by computer software, while the collaboration of other components is controlled by signals of the synchronizer. The timing diagrams of the exposure of the CCD and the laser output of the pulse laser can be adjusted according to the purpose of measurement. The laser beam is transformed to a sheet with a cylindrical lens. The nanoparticle generator is driven by high pressure gas, and the output particle concentration can be adjusted precisely by the driving pressure. While measuring the flow field with NPLS, the nanoparticles are injected into and mix with the inflow of the flow field while the flow is established in the observing widow. The synchronizer controls the laser pulse and CCD to ensure synchronization of the emission of scattering laser by nanoparticles and the exposure of CCD.

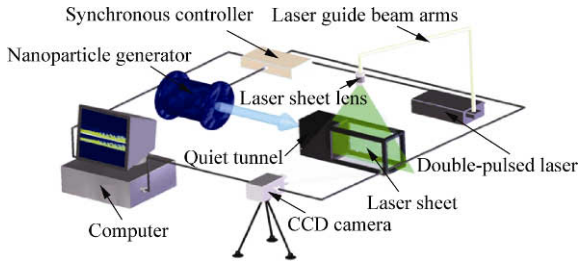

Fig. 2 Schematic of NPLS experiment system [13].

2.3. Configuration and parameters of VG

The supersonic boundary layer is generated by a plane glass, which makes it convenient to visualize the flow field. The VG is installed on a plane glass, as shown in Fig. 3. In this paper, the intensity and action range of the vortex and the height of the vortex core are considered as the reference dimensions to define the height of VGs. Figure 4 shows the schematic of VG configurations and the illuminated position of the laser sheet. The dimensions of the flat plate are as follows: 500 mm in length, 196 mm in width for plane glass; for the VG, height h = 5.8 mm, gradient a = 15°, sides C = 27 mm and half conical angle A_p=36°; the leading edges of the VGs and plane glass are parallel, with a distance of 130 mm (choosing the quiet wind tunnel's inlet as the reference point); h/δ=1.5 with δ being the thickness of the supersonic boundary layer. In the NPLS experiments, the laser sheet illuminates the symmetry plane of the VG just above the upper observation window, which is vertical to the CCD camera to observe the flow.

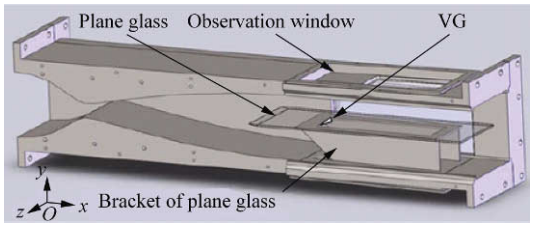

Fig. 3 Schematic of experimental installation.

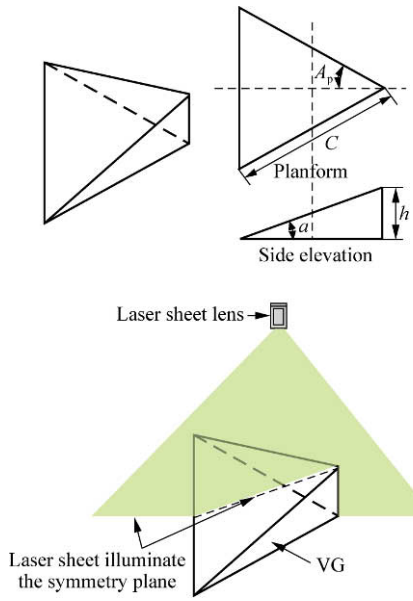

Fig. 4 Schematic of VG configurations and illuminated position of the laser sheet.

3. Spatial Vortical Structure and Evolution of Supersonic VGs

Figure 5 is the NPLS image of the supersonic laminar boundary layer along the flow symmetry plane. The distance from the front-end of the image to the leading edge of the plane glass is 300 mm, and the actual length of image is 200 mm. The image shows that the dark strap indicates the region of supersonic laminar boundary layer, and no transition is observed. The full plate boundary layer remains laminar, which means that the supersonic wind tunnel can provide supersonic flow field with high quality, little disturbance of noise wave, and low pressure fluctuation.

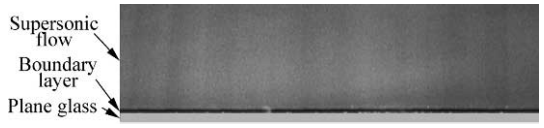

Fig. 5 NPLS image of supersonic laminar boundary layer.

The spatial feature of the supersonic laminar flow field is very sensitive to the condition of the initial value and boundary value. Even a little disturbance can cause a change of the boundary layer. The VG is fixed on the wall of the glass plane, which will cause strong interference and the disturbing signal is magnified gra-

dually during the transmission to downstream. Therefore, complicated vortical structures will be induced.

Figures 6-7 show the NPLS images of the VG symmetry plane (streamwise plane) flow field, with time sampling interval 0.5 s, stride frame time 1 μs and 20 μs, respectively. Each experiment takes sampling ten times, each sampling takes two frames of images, and maintains the same experiment conditions for the samplings of each cross-frame time. The experiments successfully indicate that the symmetry plane field structure of the VG of each sampling is distinct, while the transition location of the supersonic laminar boundary layer, the geometric configuration of vortices and their intensity vary with the different sampling time. This study further shows the non-stationarity of a supersonic laminar flow field under the action of VG. However, the spatial vortex structures demonstrate very good periodicity and similar geometric structures which are images of two continuous frames collected in an instant. When the stride frame time is 1 μs, streamwise displacement of the large vortex is very short and the configuration change is very small. When the stride frame time is 20 μs, streamwise displacement of the large vortex is very obvious, but the shape remains. The experiment results show that the structure of vortices has the characterristic of moving rapidly, and changing slowly, and large numbers of coherent vortical structures exist in the symmetric plane flow field of the VG.

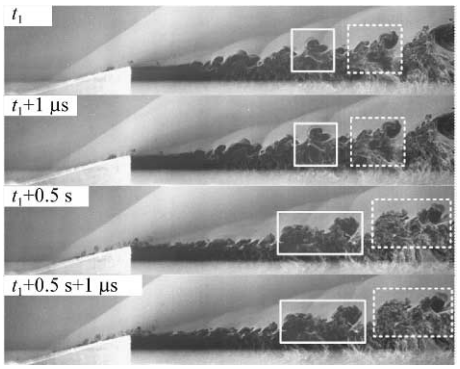

Fig. 6 Streamwise vertical structure images of the VG symmetry plane flow field (time sampling interval 0.5 s, stride frame time 1 μs).

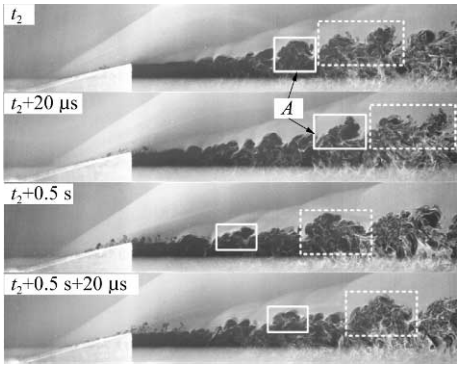

Fig. 7 Streamwise vortical structure images of the VG symmetry plane flow field (time sampling interval 0.5 s, stride frame time 20 μs).

Two strong shocks in the leading and trailing edges of the VG can also be observed in the NPLS images. The wake flow appears to be large scale coherent structures, and increases in a low velocity in the normal plate glass, which coincides with the conclusions provided by Ref. [9], which adopted the techniques of schlieren, oilflow, wall pressure's measurement, LDA, and so on. The supersonic laminar flow field causes the shear flow or vorticity under the action of the VG, which then generates instable waves, and the instable waves grow and roll up to form vortices. These random structures or relatively small vortical structures interact with each other, forming the regular large eddies which keep moving under the driving of high speed mainstream, and gradually dissipate. The movement and interacttion of vortices play an important role in the transportation of turbulence kinetic energy on the spatial scale, which will promote the external potential flow and carry it to the inside of the boundary layer, and possibly induce the burst out of the boundary layer bottom.

Figure 8 shows the local vortical structure images of the VG symmetry plane flow field with stride frame times of 5 μs and 15 μs separately. From the images, the evolution of the spatial vortical structure and the position of the vortex can be measured. According to the evolution of the vortical structure with different stride frame times, the rotation direction and deformation characteristics of the vortical structure can be defined. The rotation direction of the vortical structure is marked as white curve. The structure rotates clockwise, which is caused by the shearing action between the mainstream and the low speed flow of the boundary layer. The labels *A* and *B* in Figs. 7-8 show obviously the stretching and distortion of the vortical structure, which is relevant to the shearing action and induction of other vortices. It can be seen from the vortex evolvements in Figs. 7-8 that the merging of vortices do not appear even for a time interval of 20 μs.

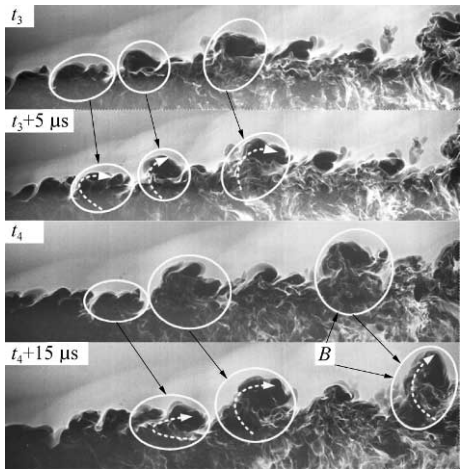

Fig. 8 Local streamwise vortical structure images of the VG symmetry plane flow field (stride frame time 5 μs and 15 μs).

4. Effect of Compressibility and Generation of Shocklet

Figure 9 shows the NPLS images of local flow vortical structures of the VG symmetry plane flow field. Large scale turbulent flow structures appear in the mainstream region, and arc shocklets emerge in the upper front of the vortical structure (marked as white curve). The strength of arc shocklets gradually weaken until finally they disappear, followed by the vortices moving downstream. Through analyzing large amounts of NPLS images, it is found that strong shock waves and expansion waves are formed at the leading, side and trailing edges of a supersonic VG, which cause a larger pressure gradient. Meanwhile, trailing vortices are formed under the action of streamwise velocity. As the airflow continuously sheds off the up-surface region at the sides and trailing edges of the VG, it continuously causes the evolving streamwise vortex. In the process of the continuous shedding and involution of a vortex, low speed flows are also involved into the high speed mainstream, and form evolving streamwise vortices with lower velocity than the local flow. Therefore, the local high speed flow will be blocked by the large scale structures, and generate evolving shocklets.

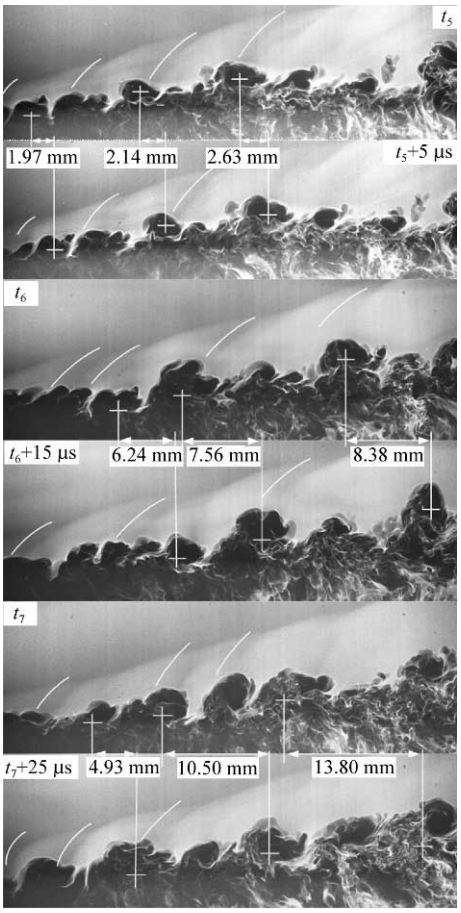

Fig. 9 Local streamwise vortical structure images of the VG symmetry plane flow field (stride frame time 5 μs,15 μs and 25 μs).

Shocklet structure is one of the most complicated phenomena in supersonic flows, which is widely studied in supersonic shear turbulence. However, there is no agreement in theory that can interpret the formation of shocklet structures [15]. At present, one explanation that receives most recognition is that when the Mach number of the mainstream relative to the Mach number of a large scale structure movement is close to or larger than 1 (the relative Mach number is larger than 1), the mainstream is hindered by the large scale structure and causes shock waves, which is called shocklets. Therefore, the convective Mach number is considered as a criterion to determine whether shocklets will be generated or not. Generally, the shocklet will not be generated until the convective Mach number is larger than 0.8 [16]. However, the definition of the convective Mach number is given under the assumption of isentropic conditions for the carrying fluid in large scale structures, while it is very difficult to determine to what extent the isentropic assumption can be satisfied for the large scale structures formed in a supersonic flow field under the action of VG, because of the strong viscous dissipation in boundary layers.

To measure quantitatively parameters of the shocklet, the NPLS images are used, with which the position and velocity of the large scale structure can be measured, and the actual convective Mach number can be computed. This method can avoid possible calculation errors due to the isentropic assumption. Figure 9 shows the NPLS images taken with a time interval of 5 μs, 15 μs and 25 μs, separately. The corresponding length of the flow field is 54 mm, the distance is 15 mm from the left of the images to the trailing edge of VG, the spatial resolution is 0.011 96 mm/pixel and the stride frame time is 0.3 μs. The white cross-line is used to locate a large vortex. Thus the streamwise distance and velocity of a large vortex can be defined. According to each stride frame time, the positions of three different large eddies are located along the streamwise, and the corresponding streamwise distance and velocity of the large vortex are obtained. The corresponding parameters are showed in Table 1.

Table 1 Streamwise distance and velocity of large vortex at different stride frame times

Stride frame time/μs	Streamwise distance/ mm	Streamwise velocity/ ($m \cdot s^{-1}$)
5	1.97	394.0
	2.14	428.0
	2.63	526.0
15	6.24	416.0
	7.56	504.0
	8.38	558.7
25	4.93	197.2
	10.50	420.0
	13.80	552.0

The velocity of the mainstream is 596.3 m/s, obtained by validation of the flow field, and the acoustic velocity is 222.4 m/s. As seen from the computation, the low speed flow in the boundary layer is accelerated

continuously by the high speed mainstream, and the velocity of the vortices increases gradually along the flow direction. The velocity of vortices is lower near the trailing edge of the VG than further downstream from the trailing edge of the VG, which is relative to the velocity of the mainstream, exceeding acoustic velocity. So the shocklet is generated in the upper front of a vortical structure. In the continuous development of the flow toward downstream, vortices are accelerated by the high speed mainstream, and the velocity of vortices becomes gradually close to the velocity of the mainstream, which causes the convective Mach number to decrease. So this is one of the causes that the intensity of a shocklet is weakened until it disappears. Figure 10 demonstrates the phenomenon.

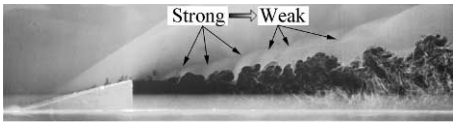

Fig. 10 Tendency chart of shocklet intensity.

To further study the shocklet by the method of quantification, experiments are performed by a supersonic PIV system. Figure 11 is the velocity field, which includes contours of the magnitude of the velocity, the velocity in x direction (streamwise) and the velocity in y direction. The distance is 14 mm from the left of the image to the trailing edge of the VG, and the corresponding length of the flow field is 36 mm, the height of the flow field is 18 mm, the spatial resolution is 0.011 96 mm/pixel and the stride frame time is 0.3 μs. It can be seen from the charts that the measuring result of velocity coincides with the vortical structure in supersonic flow around VG.

In Fig. 11, there is little difference between the contour of velocity in x direction and the resultant velocity, which indicates that the movement in x direction is predominant in the whole flow field and it plays an important role in the control of flow structure, and defines two points (marked with cross-lines) in the contour of x direction velocity. The computed result shows that the relative Mach number of the points is 1.349, which is greater than 1 and meets the condition of generating shocklets. And the mainstream passes through the shocklet, which causes the mainstream velocity to decrease. The contour of velocity in y direction shows that the upward maximum velocity is 210 m/s and the downward maximum velocity is 150 m/s. However, the downward velocity is lager than the upward velocity, which indicates that the downward overturn velocity of the mainstream is higher than the upward roll-up velocity of the low speed flow in the lower layer. The reason is that the mainstream has higher density and moves faster, which carries more energy and momentum. The mainstream transfers the energy and momentum to the low speed flow, which is helpful to enhance the mixing between the mainstream and the low speed flow. At the same time, the low speed flow and vortical structures have a tendency of ascending along streamwise direction. From Fig. 11, it can also be seen that the shocklet is slower than the vortical structures, as has been pointed out by the motion shock wave theory.

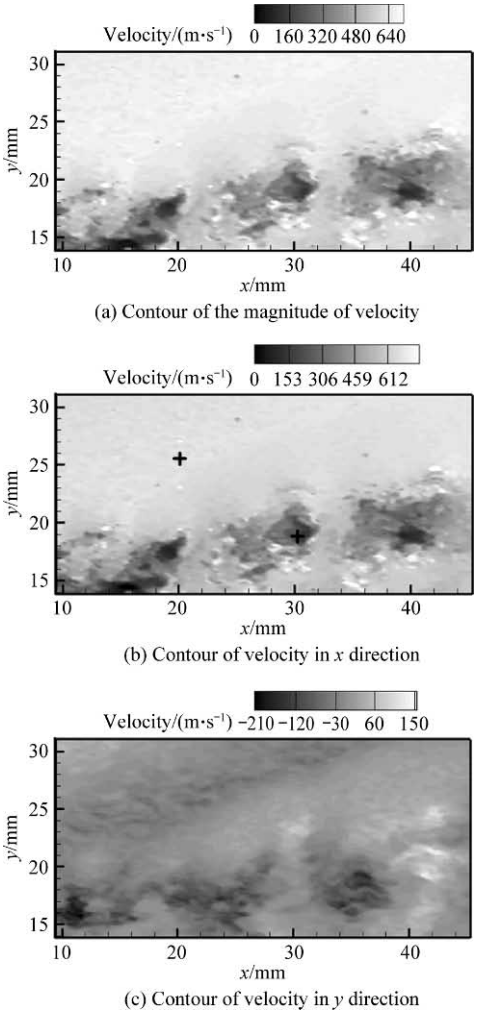

Fig. 11 Measuring results of velocity field.

In summary, the factors that cause the relative Mach number decrease can be attributed as follows:

1) When moving downstream, the vortical structure is accelerated continuously by the mainstream velocity;

2) The mainstream is decelerated by previous shocklet;

3) Along the downstream of the VG, the flow field changes into a non-isentropic contraction duct, which slows down the supersonic external flow and weakens the local shocklet intensity along the downstream of the VG.

Finally, the results indicate that shocklets will be generated in supersonic VG flow when the relative Mach number between the mainstream and the vortexes is greater than 1. But just according to the experimental results of one kind of VG in supersonic flow, it is difficult to conclude that the conditions of generating shocklets are similar.

5. Conclusions

The fine space-time structures of a supersonic boundary layer under the action of VGs are studied based on the NPLS. The vortical structures and their evolution are imaged, which shows that the coherent structures of the flow field around the VGs are unsteady. However, the vortices reveal periodic evolution and similar geometry, with characteristics of rapid translating and slow transforming. Shocklets are found in the trailing vortices of VGs, which intersect with the induced shock wave of the VG wake flow. Quantitative measurements show that the trailing vortices are rolled up from the boundary layer, and the relative velocity of vortices to the mainstream is close to or exceeds the local sonic speed, which induces the arc shocklets.

References

[1] Lin J C. Review of research on low-profile vortex generators to control boundary-layer separation. Progress in Aerospace Science 2002; 38(4-5): 389-420.
[2] Kupper C, Henry F S. Numerical study of air-jet vortex generators in a turbulent boundary layer. Applied Mathematical Modelling 2003; 27(5): 359-377.
[3] Casper M, Kähler C J, Radespiel R. Fundamentals of boundary layer control with vortex generator jet arrays. AIAA-2008-3995, 2008.
[4] Watterson J K, Leslie M, McEwan W, et al. Influence of sub-boundary layer vortex generators on wall shear stress. AIAA-2005-4649, 2005.
[5] Angele K P, Grewe F. Instantaneous behavior of streamwise vortices for turbulent boundary layer separation control. Journal of Fluids Engineeering 2007; 192(2): 226-235.
[6] Ola L, Angele K, Alfredsson P H. On the robustness of separation control by streamwise vortices. European Journal of Mechanics-B/Fluids 2010; 29(1): 9-17.
[7] Babinsky H, Ogawa H. SBLI control for wings and inlets. Shock Waves 2008; 18(2): 89-96.
[8] Berry S A, Nowak R J, Horvath T J. Boundary layer control for hypersonic airbreathing vehicles. AIAA-2004-2246, 2004.
[9] Charles W, Ford P, Babinsky H. Micro-ramp control for oblique shock wave/boundary layer interactions. AIAA-2007-4115, 2007.
[10] Lee S, Loth E, Wang C. LES of supersonic turbulent boundary layers with μVG's. AIAA-2007-3916, 2007.
[11] Blinde P L, Humble R A, van Oudheusden B W, et al. Effects of micro-ramps on a shock wave/turbulent boundary layer interaction. Shock Wave 2009; 19(6): 507-520.
[12] Anderson B H, Tinapple J, Surber L. Optimal control of shock wave turbulent boundary layer interactions using micro-array actuation. AIAA-2006-3197, 2006.
[13] Zhao Y X. Experimental investigation of spatiotemporal structures of supersonic mixing layer. PhD thesis, National University of Defense Technology, 2008. [in Chinese]
[14] Zhao Y X, Tian L F, Yi S H. Supersonic flow imaging via nanoparticles. Science in China: Series E 2009; 52(12): 3640-3648.
[15] Rossmann T. An experimental investigation of high compressblity mixing layers. Technical Report TSD-138, 2001.
[16] Kourta A, Sauvage R. Computation of supersonic mixing layers. Physics of Fluids 2002; 14(11): 3790-3797.

Biographies:

WANG Dengpan is a Ph.D. candidate. His main research interest is experimental investigation of supersonic flow control.
E-mail: wdp_1981@126.com

XIA Zhixun is a professor. His main research interests are solid rocket ramjet technology, integration technology of hypersonic vehicles and water ramjet technology.
E-mail: xiazhixun@sina.com

ZHAO Yuxin is an associate professor. His main research interest is supersonic and hypersonic experiment hydrodynamics.
E-mail: zyx_nudt@yahoo.com.cn